Nanoscale

Layered Titanium Diboride: Towards Exfoliation and Electrochemical Applications

Journal:	*Nanoscale*
Manuscript ID:	NR-ART-04-2015-002692.R1
Article Type:	Paper
Date Submitted by the Author:	29-May-2015
Complete List of Authors:	Lim, Chee Shan; Nanyang Technological University, Chemistry and Biological Chemistry Sofer, Zdenek; Institute of Chemical Technology, Prague, Department of Inorganic Chemistry Mazanek, Vlastimil; Institute of Chemical Technology, Prague, Department of Inorganic Chemistry Pumera, Martin; Nanyang Technological University, Chemistry and Biological Chemistry

Journal Name

ARTICLE

Layered Titanium Diboride: Towards Exfoliation and Electrochemical Applications

Received 00th January 20xx,
Accepted 00th January 20xx

DOI: 10.1039/x0xx00000x

www.rsc.org/

Chee Shan Lim[a], Zdeněk Sofer[b], Vlastimil Mazánek[b], Martin Pumera*[a]

Layered transition metal diborides (TMDB), amongst the other refractory metal borides, are more commonly employed for material fabrication such as wear- and corrosion-resistant coatings due to their impressive chemical stability and thermal conductivity. In spite of the wide scope of studies carried out on TMDB in the physical field, investigations on its electrochemistry remain limited. Since the physical properties play a vital role in any material's electrochemical behaviour, we explore the viability of the most popular form of titanium boride, layered TiB_2, in catalyzing electrochemical energy applications including hydrogen evolution and oxygen reduction. Three types of TiB_2 were compared in this work, those modified with sodium naphtilide and butyllithium respectively in attempt to exfoliate TiB_2 and the unmodified TiB_2. Electrocatalytic activity displayed by all three TiB_2 materials offers a wider range of opportunities for the application of TiB_2 in material studies.

Introduction

The environmental drawbacks of using the already-limiting fossil fuels to provide energy for the ever-growing world population has led to rousing impetus to create alternatives sources of clean and renewable energy.[1,2] Renewable energies in the wind and solar forms have been converted and implemented into energy storage systems for instance,[3,4] while photoelectrochemical water-splitting has also prevailed recently as a clean and environmental-benign method to store energy resources.[5,6] One of the key processes of water-splitting is proton reduction at the cathode, also known as hydrogen evolution reaction (HER).

Hydrogen is known to possess the largest current density and can be applied in many areas including fuel cells and for energy storage. Hydrogen evolution involves the reduction of protons, but often requires the help of an additional catalyst due to its sluggish kinetics which involves the adsorption of the protons onto the electrode surface followed by the desorption of molecular hydrogen. As a result, the rate of hydrogen evolution is largely dependent on the type of catalyst used, and platinum has been affirmed as the best HER catalyst by far.[7,8] This can be attributed to the very small free energy of adsorption value, ΔG_H of close to 0 which implies a fast rate of reaction.[9,10] The catalytic ability of platinum has been proven in many earlier studies, where only a small overpotential was required to activate HER. However, the cost and rarity of platinum has sparked intensive research for cheaper and more readily available substitutes. Many viable alternatives have been proposed, the more promising ones include graphene,[11,12] metal-based materials,[13,14] as well as transition metal dichalcogenides[15,16,17] which are in the centre of focus for catalyzing HER lately.

Transition metal borides including cobalt and nickel have been widely used in physical and chemical applications for their considerable advantages in electrical conductivity and hardness.[18,19,20] Specifically, transition metal diborides with a general formula of AB_2 exhibit layered structures with several properties including high thermal stability and outstanding mechanical properties. Such properties are largely dependent on the metallic ion forming the boride. Of which, MgB_2 was intensively investigated due to its high superconducting transition temperature of 39 K.[21]

Titanium borides are one of the commonly explored metal borides due to various forms ranging from TiB, Ti_2B to TiB_2. Their remarkable properties such as high chemical stability, excellent refractory properties and outstanding thermal conductivity have led to increased interest in employing them for high temperature applications.[22,23] Other than the bulk compounds, research has recently been dedicated to their counterparts on a nanoscale as well, including nanowires and nanotubes.[24] Amongst the forms of titanium boride, there has been heightened interest in developing uses for TiB_2. This is mainly due to its high stability, as previous studies have proved that the electronic densities of state for TiB_2 at the Fermi level is the lowest among the three forms.[23] On top of that, TiB_2 has also been recognized for its high strength, durability and resistance to erosion,[25,26] properties which are likely attributed

[a] School of Physical and Mathematical Science, Division of Chemistry and Biological Chemistry, Nanyang Technological University, 21 Nanyang Link, Singapore. Email: pumera.research@gmail.com
[b] Institute of Chemical Technology, Department of Inorganic Chemistry, Technická 5, 166 28 Prague 6, Czech Republic.
† Footnotes relating to the title and/or authors should appear here.
Electronic Supplementary Information (ESI) available: [details of any supplementary information available should be included here]. See DOI: 10.1039/x0xx00000x

to the simultaneous existence of metallic, ionic and covalent character in this boride compound. These exceptional

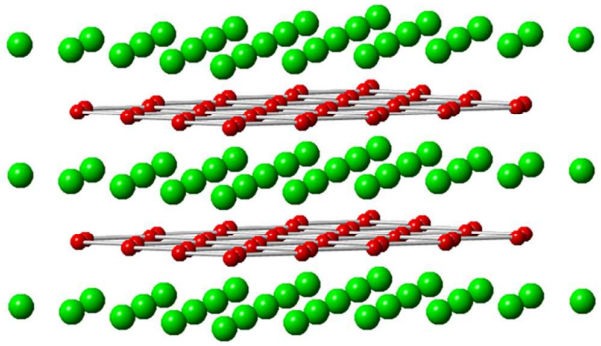

Figure 1 The structure of TiB_2 with hexagonally arranged boron atoms (red) and planes of Ti atoms (green).

characteristics have led to extensive use of TiB_2 in specialized applications such as wear-resistant coatings, cutting tools, corrosion-resistant electrical switch interfaces and even extraction of aluminium.[23,27] TiB_2 and its composites with metals or ceramic can also be applied as ballistic protection materials,[28,29] while TiB_2 coating can provide significant improvement in tribological properties of titanium.[30]

A typical polycrystalline TiB_2 can be synthesized *via* numerous methods generally form the elements by solid state reactions. The compaction is realized by several methods ranging from hot isostatic pressing,[31] microwave sintering[32] to dynamic compaction.[33] In the past decade, a novel solvothermal method was also discovered for the synthesis of TiB_2.[34] TiB_2 exhibits a hexagonal structure with a symmetry group P6/mmm as illustrated in Figure 1, where the boron atoms are hexagonally arranged in layers like carbon in graphite and exist alternately with the titanium layers.[23,27]

Despite the undeniable potential of TiB_2 in physics and material applications, inadequate investigations have been carried out on its electrochemical behaviour. Therefore, we wish to explore the electrochemistry of TiB_2 through its ability to catalyze hydrogen evolution (HER) and another common energy application involved in metal-air battery and energy storage systems, oxygen reduction reactions (ORR).[35,36] TiB_2 before treatment and after treatment with butyllithium and sodium naphtilide respectively were investigated in this work. These alkali metal compounds are typically used for intercalation of layered materials like transition metal dichalcogenides. The samples are termed as TiB_2, TiB_2/NaNAFT and TiB_2/BuLi where the terms represent the different reagents used for treatment, if any. Effects of the modified pathways on the electrochemical behaviors of the three TiB_2 were also compared on top of the general electrochemical studies aforementioned.

Experimental

Materials

Nafion 117 solution, platinum on graphitized carbon, sulfuric acid (95-98 %, v/v), potassium hydroxide, sodium chloride, potassium chloride, sodium phosphate dibasic and potassium phosphate monobasic were obtained from Sigma-Aldrich, Singapore. Titanium diboride, n-butyllithium (2.5 M in hexane), benzophenone and sodium were obtained from Sigma-Aldrich, Czech Republic. Naphthalene, tetrahydrofurane (THF), hexane and methanol were obtained from Lach-Ner, Czech Republic. Argon (99.996 %) was obtained from SIAD, Czech Republic. THF was dried prior to use by distillation from sodium/benzophenone mixture under argon atmosphere. Glassy carbon (GC) electrodes with a diameter of 3 mm were obtained from Autolab, The Netherlands. Milli-Q water with a resistivity of 18.2 MΩ.cm was used throughout the experiments.

Synthesis and Procedure

TiB_2/NaNAFT was synthesized by reaction of TiB_2 with sodium naphtilide in THF. 2 g of sodium and 0.5 g of TiB_2 was placed in 250 mL flask with 100 mL of dry THF. Subsequently, 12 g of naphthalene was added and the reaction mixture was heated under reflux for 24 hours under argon atmosphere. TiB_2 was speared by suction filtration under argon atmosphere, and repeatedly washed with dry THF before re-dispersing in methanol. The suspension was then filtered by suction, washed with water and dried in a vacuum oven for 48 hours at 50 °C before further use.

TiB_2/BuLi was synthesized by the reaction of TiB_2 with butyllithium. 0.5 g of TiB_2 was placed in a 100 mL flask and 25 mL of 2.5 M butyllithium in hexane was added. The reaction mixture was stirred under argon atmosphere for 48 hours. TiB_2 was separated by suction filtration and repeatedly washed with hexane. The whole procedure was performed in the glove box with argon atmosphere. Following which, TiB_2 was removed from the glove box, dispersed in methanol. The suspension was suction filtered, washed with water and dried in vacuum oven before further use (48 hours, 50 °C).

Cyclic voltammetry measurements were performed using a scan rate of 100 mV s^{-1} for inherent electrochemistry scans. Linear sweep voltammetry measurements were recorded at a scan rate of 2 mV s^{-1} for HER and 5 mV s^{-1} for ORR. 0.5 M sulfuric acid was used as the electrolyte for HER, whereas 0.1 M potassium hydroxide functioned as the electrolyte for ORR. Reproducibility of the measurements was ensured by obtaining three replicates for each experiment.

A suspension of the desired material with a concentration of 5 mg mL^{-1} in respective solvent mixtures was first prepared, followed by a 60 min ultrasonication. DMF is used as the solvent to disperse the material for HER; water suspension with 0.1 wt% nafion solution was used as the solvent for ORR experiments. A micropipette was then used to deposit 1 µL aliquot of the respective suspension onto the electrode surface to immobilise the material onto the working electrode. The solvent was allowed to evaporate at room temperature to obtain an evenly distributed film on the electrode surface. To renew the electrode surfaces, polishing was done with 0.05 µm alumina powder on a polishing pad.

Instrumentation

Scanning electron microscopy (SEM) was carried out with a FEG electron source (Tescan Lyra dual beam microscope) to obtain the morphology of the borides. Energy dispersive spectroscopy (EDS) as performed with an analyzer (X-Max^N) with a 20 mm^2 SDD detector (Oxford instruments) and AZtecEnergy software to acquire the elemental composition and mapping. To conduct the measurements, the samples were placed on a carbon conductive tape. SEM and SEM-EDS measurements were carried out using a 15 kV electron beam. X-ray powder diffraction (XRD) data were collected at room temperature with an X'Pert PRO θ-θ powder diffractometer with parafocusing Bragg–Brentano geometry using CuKα radiation (λ = 0.15418 nm, U = 40 kV, I = 30 mA). Data were scanned with an ultrafast detector X'Celerator over the angular range 5 - 80° (2 θ) with a step size of 0.0167° (2θ) and a counting time of 20.32 s step^{-1}. Data evaluation was performed in the software package HighScore Plus.

X-ray photoelectron spectroscopy (XPS) measurements were recorded using a Phoibos 100 spectrometer and a monochromatic Mg X-ray radiation source (SPECS, Germany). Survey scans and high-resolution spectra of the borides were used to determine the surface composition of the materials. The boride samples were prepared by fixing the material onto an aluminium XPS sample holder using a sticky conductive carbon tape. A uniform layer of the material was ensured throughout.

Linear sweep voltammetry (LSV) and cyclic voltammetry (CV) measurements were carried out with a µAutolab type III electrochemical analyser (Eco Chemie, The Netherlands) connected to a personal computer and controlled by NOVA 1.10 software. Experiments were performed in a 5 mL electrochemical cell with GC electrodes using a three-electrode configuration at room temperature; a platinum electrode was used as a counter electrode while an Ag/AgCl electrode functioned as a reference electrode. All electrochemical potentials in this work are presented *vs.* the Ag/AgCl reference electrode unless otherwise stated.

Results and Discussion

Characterisation of the three TiB_2 samples was carried out to evaluate possible structural and composition differences prior to electrochemical studies.

Scanning electron microscopy was first employed to study the morphological differences upon various modifications of the obtained TiB_2. Smooth particles, mostly rounded, were apparent in the unmodified TiB_2 sample as displayed in Figure 2A. Modification with the sodium naphtilide did not result in major changes in the particles, other than the size where the modified TiB_2/NaNAFT exhibited particles of larger size, with evident layers observed along the edges (Figure 2B). Finally, particles with irregular and less rounded shapes, accompanied with a small degree of cracks and sharp edges were observed for the BuLi–modified sample, as illustrated in Figure 2C. In general, the morphologies of the three samples did not show significant discrepancies, as they possess relatively smooth surfaces with lengths of a few micrometers.

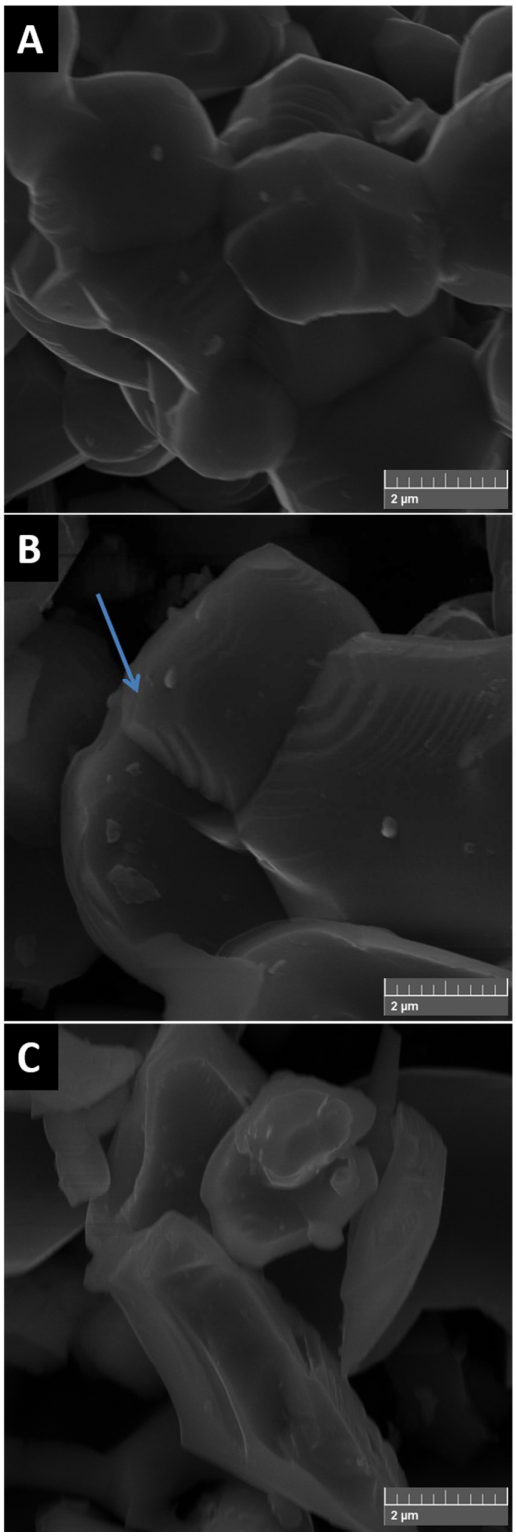

Figure 2 SEM images of (A) TiB_2, (B) TiB_2/NaNAFT and (C) TiB_2/BuLi at magnifications of 5,000 x respectively. Scale bar: 2 µM

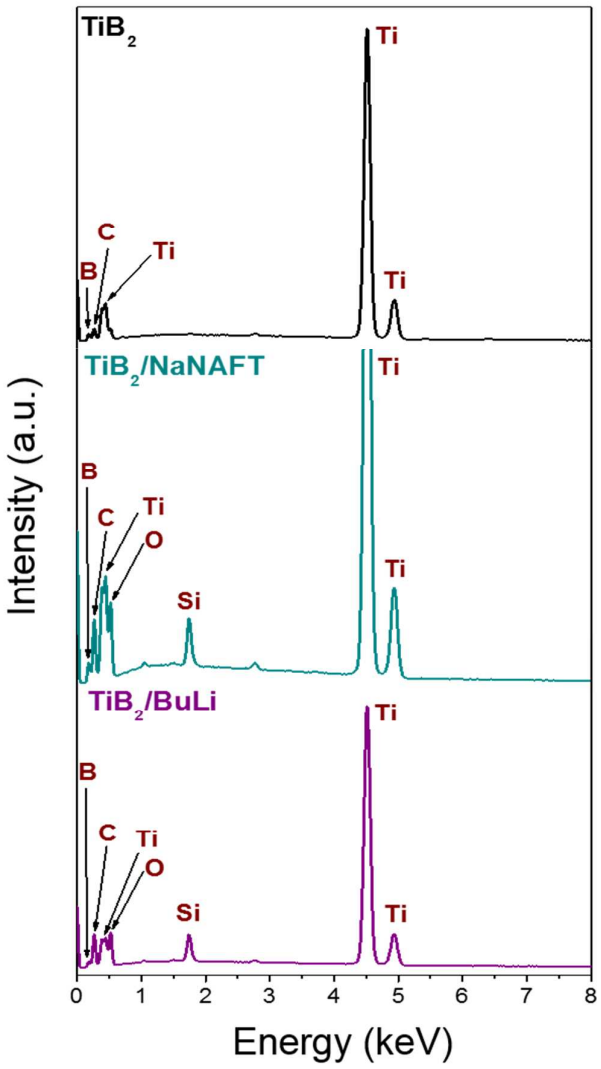

Figure 3 Energy-dispersive X-ray spectroscopy (EDX) spectra of titanium diborides.

Energy-dispersive spectra of the three samples were also performed in order to obtain a rough gauge of the elemental compositions. Figure 3 displays a direct comparison of the three samples, and the spectra appear to be almost identical, with prominent titanium signals observed. Boron peaks were almost negligible, however, most like due to low sensitivity of EDS towards light elements, as well as possible inherent physical and technical limitations of the equipment. Carbon impurities were observed for all samples, which can be attributed to adventitious carbon present during the measurement. Other impurities including oxygen and silicon were also detected, but they were only prominent in the modified TiB_2 samples, suggesting possible existence during the synthesis processes.

The phase purity and structure was further confirmed by X-ray diffraction. No significant differences were observed between TiB_2 before and after treatment with the exfoliation agents. However slight decrease of the (001) intensity (at 27.54°) could possibly imply partial etching of layers by sodium naphtilide. In addition, a small concentration of TiN originating from starting material was observed as well. The concentration of TiN is about 3 wt% and no other changes were observed on the samples following the treatments with sodium naphtilide or butyllithium respectively. The results of X-ray diffraction are shown on Figure 4.

X-ray photoelectron spectroscopy was subsequently carried out to study the surface composition as well as the binding environments of the samples for further verification of the materials. Survey scans in Figure 5A exhibit matching spectra for all three samples, with carbon and oxygen peaks detected other than the main titanium and boron signals. Positions of the peaks were also almost identical, denoting similar chemical environments experienced by the elements in the samples. High-resolution spectra for Ti 2p and B 1s were then analysed for clearer comparison. For the Ti 2p spectra (Figure 5B), a pair of spin-orbit coupling peaks were observed for all three samples, with a spin-orbit splitting value, δ of about 5.7 eV. In addition, the $2p_{3/2}$ peaks were located at similar binding energies of 458.4 eV, 457.8 eV and 457.8 eV for TiB_2, TiB_2/NaNAFT and TiB_2/BuLi respectively. These values and peak positions concur largely with the oxidised form of TiB_2 in previous studies, indicating possible oxidation of the samples at the surface;[37,38] this attribution is also supported by the apparent O 1s peaks recorded in the survey scans. Nonetheless, the consistencies of the two modified samples with the initial TiB_2 signify successful syntheses of the former despite a small downward shift (~0.6 eV) of the $2p_{3/2}$ peaks for the modified samples. One broad B 1s signal was also apparent in all three spectra, as shown in Figure 5C. The 1s signals were positioned at approximately 192.1 eV, with deviations of only 0.1 eV. However, the B 1s signal was most prominent in the TiB_2 sample, suggesting possible diminishing of boron upon modifications. Despite so, the 1s peak positions are in good agreement to that obtained for typical surface oxidised titanium diborides, hence affirming successful synthesis.

With the titanium diboride samples characterised, electrochemical behaviour and catalytic properties were subsequently analysed.

The inherent electrochemistry of the three samples were first studied to ascertain any electrochemically oxidisable or reducible surface species. No evident signals were observed for all three samples, as displayed in Figure 6, suggesting limited electrochemical redox of TiB_2 in nature. Nonetheless, slight oxidation of the samples was still noticed at around –0.7 V; this indicates possible oxidisable species in the samples, albeit in negligible presence. Other than that, there is a general absence of innate oxidisable and reducible functionalities in TiB_2.

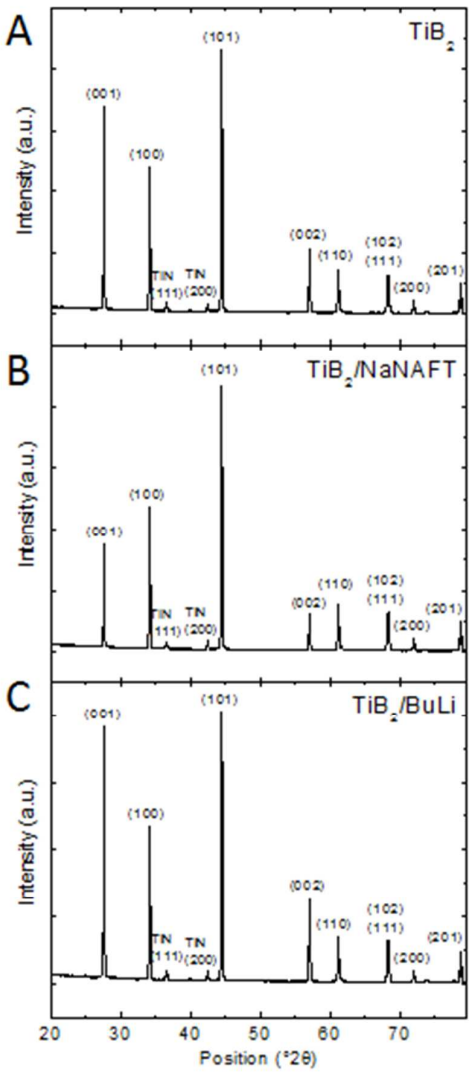

Figure 4 X-ray diffractograms of (A) TiB_2, (B) TiB_2/NaNAFT and (C) TiB_2/BuLi.

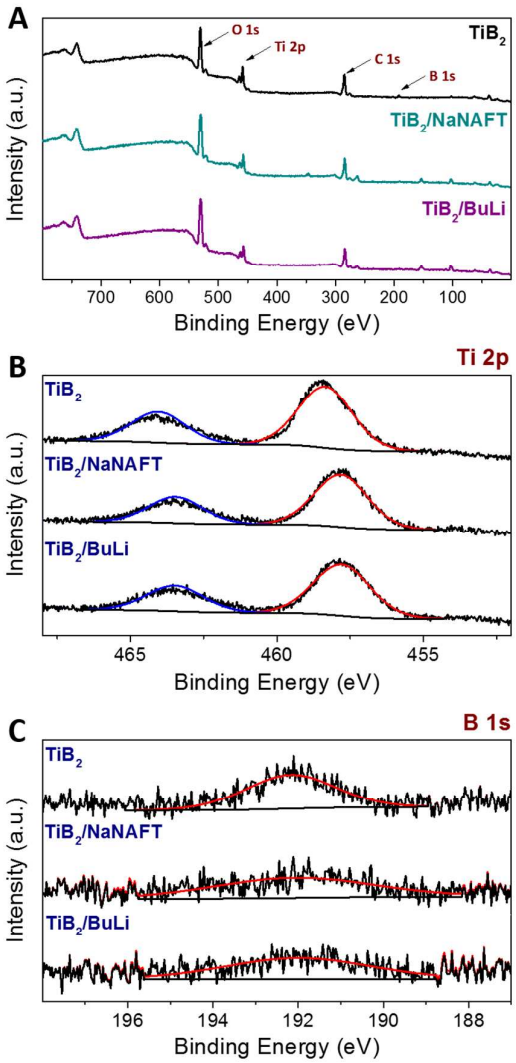

Figure 5 (A) Survey scan (top row) and (B, C) high resolution spectra of TiB_2.

The electrochemical properties of the diboride materials were first investigated through their ability to bring about fast heterogeneous electron transfer (HET). Potassium ferro/ferricyanide was employed for this study due to the surface-sensitive nature of the redox probe, and the results are displayed in Figure 7A. Further information on the peak-to-peak separation was extracted and summarized in Figure 7B, for the quantification of HET rate. Of the three diboride materials, the untreated TiB_2 induced the fastest HET rate at about 1.32×10^{-4} cm s^{-1}. On the contrary, the two modified TiB_2 surfaces were inferior in stimulating electron transfer compared to the bare GC surface. While TiB_2 indeed exhibited electrochemical activity in enhancing HET rates with reference to the bare GC surface, modifications might have resulted in loss of some electrochemical properties that are responsible for this reactivity. In general the treatment with BuLi and NaNAFT led to partial etching and cleaning of TiB_2 surface. This is documented by SEM, where we can see the layered

structure of TiB_2. This treatment slightly influenced electrochemical properties such as HET rate.

Following the establishment of the inherent electrochemical behaviour, electrocatalytic capabilities of the TiB_2 samples were investigated and compared using hydrogen evolution reaction. While onset potential is a good indication of the activity of a possible catalyst, it is not the most accurate due to absence of a specific point of comparison. A more precise analysis is the comparison of the overpotential required for the current density value to reach –10 mA cm^{-2}, a magnitude equivalent to 12.3 % efficiency of a solar-to-hydrogen conversion device.[10] As illustrated in Figure 8A, TiB_2/NaNAFT and TiB_2/BuLi required the smallest amount of overpotential (~1 V) whereas an overpotential of close to 1.1 V was necessary for the unmodified TiB_2 to attain the desired current density value. It is mentionable that as the current density increased, instability was evident for TiB_2 as the increment was not smooth and steady. As a result, modifications to the original TiB_2 sample might suggest an enhancement in stability of the material upon hydrogen evolution.

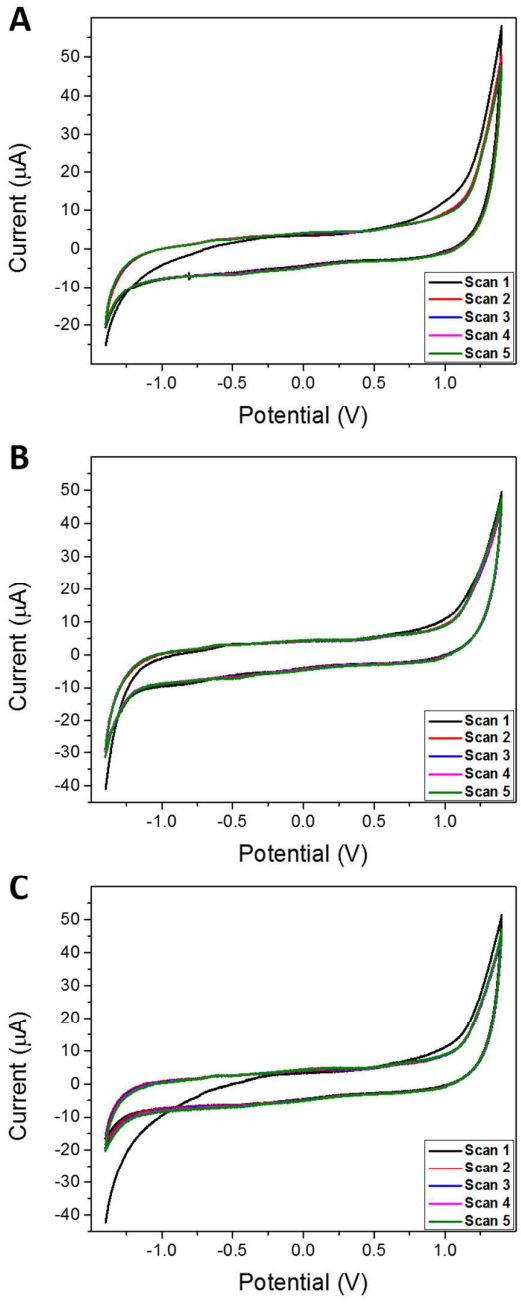

Figure 6 Cyclic voltammograms of (A) TiB_2, (B) TiB_2/NaNAFT and (C) TiB_2/BuLi in the anodic direction in PBS background electrolyte (50 mM, pH 7.2). Scan rate: 100 mV s^{-1}.

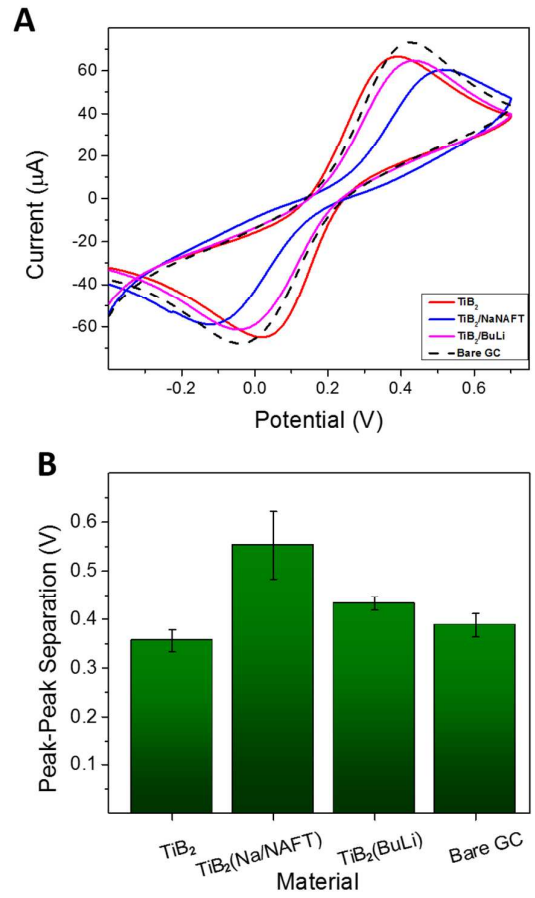

Figure 7 (A) Cyclic voltammograms of titanium diborides against bare GC surface in 10 mM potassium ferro/ferricyanide and (B) their respective peak-to-peak separation. Scan rate: 100 mV s^{-1}.

Tafel slope was the next parameter used to affirm the electrocatalytic abilities of the TiB_2 materials. Comparison of the Tafel slopes in Figure 8B shows that TiB_2/NaNAFT and TiB_2 generated the smallest slope of about 146 mV/dec, followed by TiB_2/BuLi with slope of 158 mV/dec. The marginal discrepancy between TiB_2/NaNAFT and TiB_2 imply that the reaction kinetics of HER are largely unaffected by the modifications. Despite their inferiority against Pt/C, the boride–modified surfaces still outperformed the unmodified bare GC surface in both parameters studied. Hence, titanium borides have been primarily established as an

electrocatalytically active material for HER, with TiB_2/NaNAFT as the best-performing material among the three materials studied.

Finally, ability of the TiB_2 materials in catalysing oxygen reduction reaction in alkaline medium is examined. Measurements were carried out in both saturated and purged potassium hydroxide systems and displayed in Figure 9A.

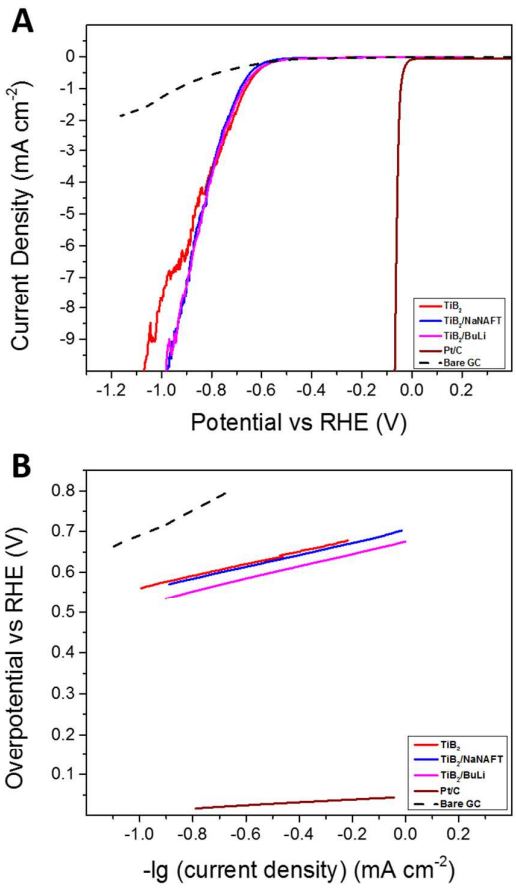

Figure 8 (A) Linear sweep voltammograms of hydrogen evolution and (B) Tafel slopes of titanium diborides against platinum and bare GC surfaces. Conditions: 0.5 M sulfuric acid, scan rate 2 mV s^{-1}.

Insignificant signals were observed for the purged system (dotted lines) while apparent reduction peaks were recorded at about –0.3 to –0.4 V in the saturated electrolyte, indicating that the peaks observed correspond to that of oxygen reduction. This is also a telling sign of the electrocatalytic activity of the diborides as all surfaces coated with the different TiB_2 materials exhibited an evident reduction peak. The extent of the ability of the diborides in catalyzing ORR was further justified by the onset potential, which was fixed at the potential when 10 % of the peak current value is reached. Other than the Pt/C–modified surface which registered the earliest onset potential of about –0.2 V, onset of ORR occurred at similar potentials for the other four surfaces. A detailed comparison shows TiB_2/NaNAFT and bare GC exhibiting slightly earlier onset potential of –276 mV, whereas TiB_2 and TiB_2/BuLi generated onset potentials of –277 and –279 mV respectively.

Conclusions

Comprehensive structural and electrochemical studies were carried out in this work in the hope of a further development of TiB_2 in the field of electrochemistry. Despite their inability to surpass the performance of Pt/C, the TiB_2 surfaces still displayed superiority over the bare GC surface in general. This is indicative of the electrochemical ability and activity of the TiB_2, which can potentially lead to further applications that require the use of cost-effective and widely available materials. Comparison results have shown very minor inconsistencies among the three titanium diborides studied; out of which, TiB_2/NaNAFT appears to be the most promising based on its potential in catalyzing hydrogen evolution. While modifications might not have resulted in remarkable differences, these findings undoubtedly shed light on the possibility of the enhancement of TiB_2 properties *via* synthetic adjustments.

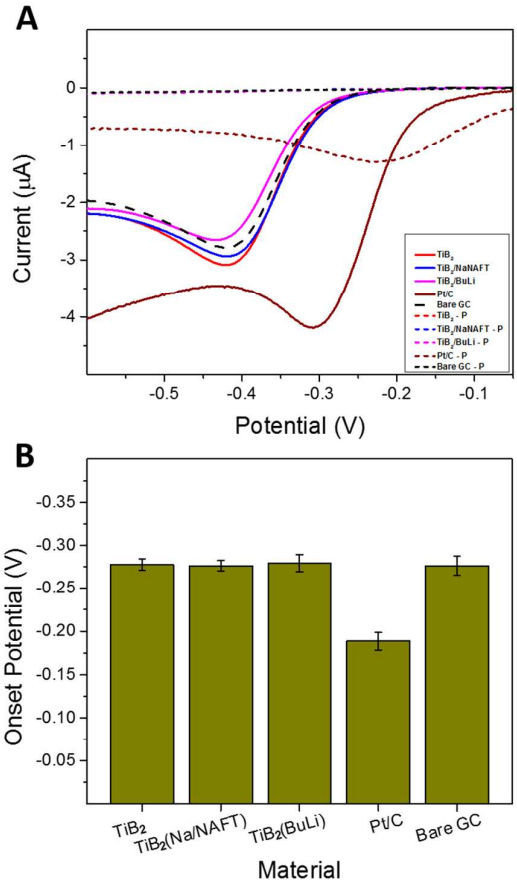

Figure 9 (A) Linear sweep voltammograms of oxygen reduction and (B) onset potentials of titanium diborides against platinum and bare GC surfaces. Conditions: 0.1 M potassium hydroxide, scan rate 5 mV s^{-1}.

Acknowledgements

M.P. acknowledges a Tier 2 grant (MOE2013-T2-1-056; ARC 35/13) from the Ministry of Education, Singapore. Z.S. and V.M. were supported by Specific University Research (MSMT No. 20/2015) and Czech Science Foundation (GACR No. 13-17538S).

Notes and references

1 D. Merki and X. Hu, *Energy Environ. Sci.*, 2011, **4**, 3878.
2 S. Chu and A. Majumdar, *Nature*, 2012, **488**, 294.
3 K. H. Solangi, M. R. Islam, R. Saidur, N. A. Rahim and H. Fayaz, *Renew. Sust. Energy Rev.*, 2011, **15**, 2149.
4 M. G. Walter, E. L. Warren, J. R. McKone, S. W. Boettcher, Q. X. Mi, E. A. Santori and N. S. Lewis, *Chem. Rev.*, 2010, **110**, 6446.
5 K. Sivula, R. Zboril, F. Le Formal, R. Robert, A. Weidenkaff, J. Tucek, J. Frydrych and M. Grätzel, *J. Am. Chem. Soc.*, 2010, **132**, 7436.
6 G. Wang, H. Wang, Y. Ling, Y. Tang, X. Yang, R. C. Fitzmorris, C. Wang, J. Z. Zhang and Y. Li, *Nano Lett.*, 2011, **11**, 3026.
7 B. E. Conway and B. V. Tilak, *Electrochim. Acta.*, 2002, **47**, 3571.
8 H. B. Gray, *Nat. Chem.*, 2009, **1**, 7.
9 R. Parsons, *Trans. Faraday Soc.*, 1958, **54**, 1053.
10 J. D. Benck, T. R. Hellstern, J. Kibsgaard, P. Chakthranont and T. F. Jaramillo, *ACS Catal.*, 2014, **4**, 3957.
11 Y. Zheng, Y. Jiao, Y. Zhu, L. H. Li, Y. Han, Y. Chen, A. Du, M. Jaroniec and S. Z. Qiao, *Nat. Commun.*, 2014, **5**, 3783.
12 P. Gao, J. Liu, S. Lee, T. Zhang and D. D. Sun, *J. Mater. Chem.*, 2012, **22**, 2292.
13 W.-F. Chen, K. Sasaki, C. Ma, A. I. Frenkel, N. Marinkovic, J. T. Muckerman, Y. Zhu and R. R. Adzic, *Angew. Chem. Int. Ed.*, 2012, **51**, 6131.
14 M. Ledendecker, G. Clavel, M. Antonietti and M. Shalom, *Adv. Funct. Mater.*, 2015, **25**, 393.
15 K. Xu, F. Wang, Z. Wang, X. Zhan, Q. Wang, Z. Cheng, M. Safdar and J. He, *ACS Nano*, 2014, **8**, 8468.
16 D. Voiry, H. Yamaguchi, J. Li, R. Silva, D. C. B. Alves, T. Fujita, M. Chen, T. Asefa, V. B. Shenoy, G. Eda and M. Chhowalla, *Nat. Mater.*, 2013, **12**, 850.
17 Y. Li, H. Wang, L. Xie, Y. Liang, G. Hong and H. Dai, *J. Am. Chem. Soc.*, 2011, **133**, 7296.
18 K.-I. Takagi, *J. Solid State Chem.*, 2006, 179, 2809.
19 T. G. Back, D. L. Baron and K. Yang, *J. Org. Chem.*, 1993, **58**, 2407.
20 A. Rinaldi, S. Licoccia, E. Traversa, K. Sieradzki, P. Peralta, A. B. Dávila-Ibáñez, M. A. Correa-Duarte and V. Salgueirino, *J. Phys. Chem. C*, 2010, **114**, 13451.
21 J. Nagamatsu, N. Nakagawa, T. Muranaka, Y. Zenitani and J. Akimitsu, *Nature*, 2001, **410**, 63.
22 L. Lu, M. O. Lai and H. Y. Wang, *J. Mater. Sci.*, 2000, 35, 241.
23 H.-Y. Yan, Q. Wei, S.-M. Chang and P. Guo, *Trans. Nonferrous Met. Soc. China*, 2011, **21**, 1627.
24 G. Kartal, S. Timur, M. Urgen and A. Erdemir, *Surf. Coat Technol.*, 2010, **204**, 3935.
25 V. I. Matkovich, *Boron and Refractory Borides*, Springer Verlag, New York, 1977.
26 W. A. Zdaniewski, J. Wu, S. C. Gujrathi and K. Oxorn, *J. Mater. Res.*, 1991, **6**, 1066.
27 R. G. Munro, *J. Res. Natl. Inst. Stand. Technol.*, 2000, **105**, 709.
28 S. Rodriguez, V. B. Munoz, E. V. Esquivel, L. E. Murr and N. L. Rupert, *J. Mater. Sci. Lett.*, 2002, **21**, 1661.
29 A. Pettersson, P. Magnusson, P. Lundberg and M. Nygren, *Int. J. Impact Eng.*, 2005, **32**, 387.
30 B. J. Kooi, Y. T. Pei and J. Th. M. De Hosson, *Acta Mater.*, 2003, **51**, 831.
31 Y. Muraoka, M. Yoshinaka, K. Hirota and O. Yamaguchi, *Mat. Res. Bui.*, 1996, **31**, 787.
32 C. E. Holcombe and N. L. Dykes, *J. Mat. Sci.*, 1991, **26**, 3730.
33 L. Wang, M. R. Wixom and L. T. Thompson, *J. Mat. Sci.*, 1994, **29**, 534.
34 Y. Gu, Y. Qian, L. Chen and F. Zhou, F. *J. Alloys and Compounds*, 2003, **352**, 325.
35 L. Qu, Y. Liu, J.-B. Baek and L. Dai, *ACS Nano*, 2010, **4**, 1321.
36 F. Cheng and J. Chen, *Chem. Soc. Rev.*, 2012, **41**, 2172.
37 G. Mavel, J. Escard, P. Costa and J. Castaing, *Surf. Sci.*, 1973, **35**, 109.
38 E. C. Onyiriuka, *Appl. Spectro.*, 1993, **47**, 35.

